

Properties of Polyhydroxy Butyrate Polyvalerate Biopolymeric Nanocomposites Reinforced with Natural Halloysite Nanotubes

Abdullah Fahim¹, Shaik Zainuddin^{1,*}, Shaik Shoieb³, Mahesh V. Hosur¹, Dawen Li³, Mackenzie Matthews² and Shaik Jeelani^{1,2}

¹Department of Materials Science and Engineering, Tuskegee University, Tuskegee, AL 36088, US

²Department of Mechanical Engineering, Tuskegee University, Tuskegee, AL 36088, US

³Department of Electrical Engineering, University of Alabama, Tuscaloosa, AL 35487, US

Abstract: In this study, the properties of bacterial fermentation based poly(hydroxybutyrate-co-hydroxyvalerate) –PHBV thermoplastic biopolymer was investigated by reinforcing natural halloysite nanotubes (HNTs). At first, HNTs were added to PHBV polymer by melt processing technique. The modified PHBV resin was then used to fabricate films using compression molding process. X-ray diffraction (XRD), differential scanning calorimetry (DSC), thermogravimetric analysis (TGA) and tensile tests were performed. XRD results showed mixed intercalated and exfoliated behavior of HNTs in PHBV matrix with an increase in interplanar spacing and decrease in peak intensity. DSC analysis showed that the crystallinity of PHBV resin increased with the increase in HNTs concentration. Also, the DSC endotherm curve showed dual melting peaks indicating formation of different crystalline phases. Higher melting and recrystallization temperature was found in nanophased samples in comparison to the pure PHBV counterpart. The thermal stability, activation energy, tensile and viscoelastic properties of nanophased samples were also increased with an optimum at 3 wt. % HNTs loading. Scanning electron micrographs (SEM) revealed river like pattern in neat films indicating a brittle failure in contrast to rougher surfaces observed in nanophased samples.

Keywords: Biopolymers, nanoparticles, thermal properties, mechanical properties, SEM.

1. INTRODUCTION

Polyhydroxy alkanones (PHAs) biopolymers are produced from renewable resources and degrade when exposed to carbon dioxide and water. In addition to PHAs natural origin, properties like biocompatibility, thermoplasticity [1] as well as the capability to emit less greenhouse gas and to generate less landfill waste made them suitable for packaging and automotive applications [2].

Among the members of PHAs family, poly(3-hydroxybutyrate) (PHB) and the copolymer poly(3-hydroxybutyrate-co-3-hydroxyvalerate) (PHBV) are the best-known types of biopolymers. The PHBV polymer is a brittle and crystalline material which consists of hydroxybutyrate (HB) content with 0-24% of hydroxyvalerate (HV) unit with a short pendent side-groups on its backbone [3]. The mechanical properties of PHBV polymer are almost similar to some polyolefins like polypropylene, which makes it an excellent alternative to many synthetic based polymers. Moreover, the biodegradability and the biocompatibility nature of PHBV polymer has given it a remarkable breakthrough in biomedical applications specifically in tissue engineering [4].

However, the mechanical strength of PHBV thermoplastic polymer is not satisfactory enough and their thermal stability is also poor [1, 4]. In addition, the slow crystallization rate restricts their use in many practical applications in large volume [5]. In recent years, the incorporation of nanofillers/nanoparticles improved the mechanical and thermal properties of various polymers [6-12]. For example, montmorillonite clay, a member of the smectite family is one of the widely used nanofiller that is used to improve multifunctional properties of the polymer such as mechanical, barrier and thermal properties, especially when good dispersion was achieved [2, 5]. Recently, halloysite nanotubes (HNTs), a member of the Kaolin group have attracted the interest as effective nanoparticles for optimizing the properties of polymers. HNTs are ultra-tiny hollow tubes similar to carbon nanotubes [1] with diameters typically smaller than 100nm and the length typically range from about 500nm to over 1.2 μ [13]. The chemical structure of HNTs is either $(Al_2Si_2O_5(OH)_4 \cdot H_2O)$ or $(Al_2Si_2O_5(OH)_4 \cdot 2H_2O)$ depending upon dehydrated (d_{001} spacing 7 Å) or hydrated (d_{001} spacing 10Å) state which is chemically related to kaolin. The external surface of HNTs is mainly composed of the siloxane (Si-O-Si) groups, whereas the internal surface consists of a gibbsite-like array of aluminol (Al-OH) groups [14]. HNTs contain two types of hydroxyl groups, which are situated on the surface of the nanotubes and in between the layers which are called inner and outer

*Address correspondence to this author at the Department of Materials Science and Engineering, Tuskegee University, Tuskegee, AL 36088; Tel: +1 334-724-4222; Fax: +1 334-724-4224; E-mail: szainuddin@mytu.tuskegee.edu

hydroxyl groups, respectively. The presence of hydroxyl groups on HNTs can form a hydrogen bonding with the polymer functional groups, and thus may favor a uniform dispersion [15, 16]. Recent studies have shown improvements in various material properties of polymers with the addition of HNTs. For example, HNTs have been used to improve the properties of regenerated cellulose, polypropylene, polystyrene, nylon 6 etc. [17-20]. Most of these studies involved in improving mechanical properties like tensile strength, stiffness; thermal properties like thermal stability, fire retardant along with improvement of electrical conductivity, moisture resistance etc. However, only a few researchers have investigated the properties of PHBV by the addition of HNTs. Other nanoparticles such as the carbon nanofibers (CNFs) and carbon nanotubes (CNTs) were also used to enhance the properties of PHBV [21]. But due to the toxic nature of the carbon based nanoparticles and the cost involved with CNTs and CNFs, we used environmentally friendly and natural HNTs in this study. We investigated the mechanical and thermal properties of PHBV nanobiocomposites modified using various percentages of HNTs. In addition, we determined the activation energy during decomposition, and also measured the crystallite dimensions of neat PHBV and PHBV/HNTs nanobiocomposites, which is to our best of knowledge, have not done before.

2. MATERIALS AND MANUFACTURING

2.1. Materials

The bacterial grade PHBV containing 12 mol% of valerite was supplied by Good fellow Cambridge Limited, UK. This material is an easily melt processible semi crystalline thermoplastic polyester (pallet form) made by biological fermentation (renewable carbohydrate feed stocks). The average size of pallets was 0.5mm. HNTs, an un modified tubular shaped clay was purchased from Natural Nano, Inc. The measured pore volume of HNT was 0.17-0.19 cc/g.

2.2. Manufacturing

At first, 1-3 wt. % of HNTs were added with the PHBV pallets and then melt mixed using a twin screw extruder machine. The extruder machine was operated at 100 rpm, and the temperature of different zone was maintained in between 145-166°C to avoid polymer and filler degradation. Finally, the solution collected from the extruder machine was compression molded in a Wabash hot press to get the nanocomposite films of 0.45-0.48mm thickness. During compression molding, a 2.5 ton force was applied for 10 min and the temperature was maintained at 166°C. Figure 1 shows the processing steps of PHBV/HNTs nanocomposite film. Neat PHBV composite films were also prepared using the same procedure for baseline comparison.

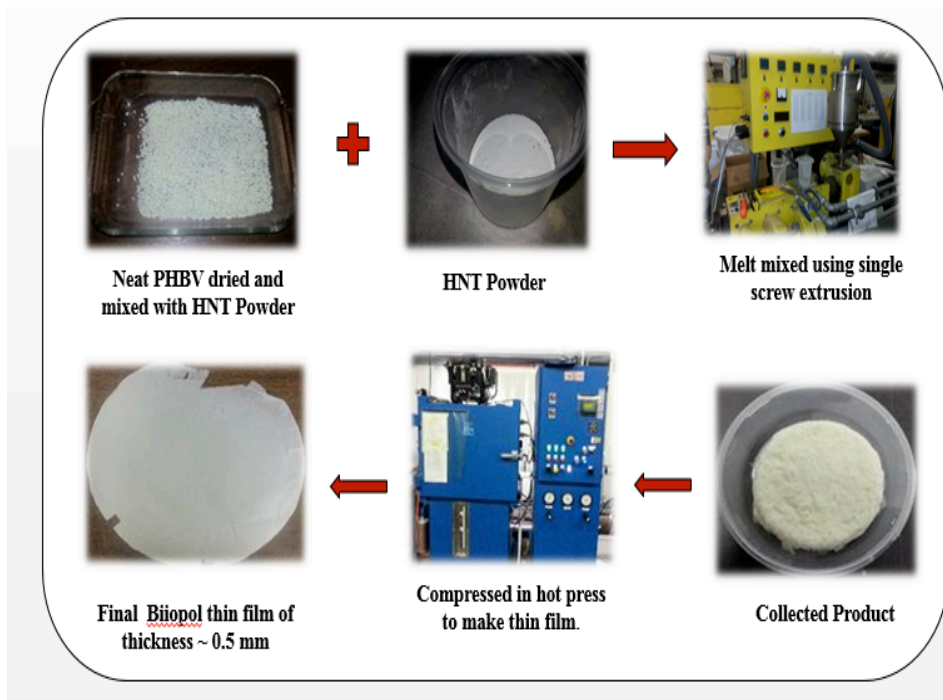


Figure 1: Fabrication of PHBV/HNTs bionanocomposite films.

3. EXPERIMENTAL PROCEDURES

3.1. X-Ray Diffraction (XRD) Analysis

XRD patterns of PHBV neat and nanophased samples were recorded by Rigaku D/MAX 2200 X-ray diffractometer with Cu K α radiation ($\lambda = 1.54 \text{ \AA}$) min. The machine was operated at 40kV and 30mA with a scanning speed of 3° per minute. During the XRD test, the samples were analyzed in the reflection mode.

3.2. Crystallinity and Crystallite Dimensions

The average crystalline size of samples was determined by Scherrer's equation [5]:

$$D = \frac{K\lambda}{\beta \cos\theta} \quad (1)$$

where, D is the average crystallite size, β is the peak width at half intensity, λ is the wavelength of X-ray radiation, θ is the diffraction angle, K is a constant which has a relation to the crystalline shape, and its value for PHBV was taken as 0.9 [22].

3.3. Differential Scanning Calorimetry (DSC) Analysis

Crystallization characteristics and melting temperature of samples were analyzed with DSC using a TA instruments Q1000. The DSC tests were carried out under nitrogen atmosphere. At first, samples were heated from 30°C to 200°C with a heating rate of 10°C/min. The samples were then held at 200°C for 5 min in order to remove the thermal history present before. Finally, the samples were cooled to room temperature at the same rate, and then again heated to a temperature of 200°C. Data were taken in the 1st cooling and in the 2nd heating cycles, respectively. The percent crystallinity of the neat and nanophased polymer was calculated using the following equation:

$$X_c = \frac{\Delta H_m}{f_p \cdot \Delta H_m^0} \times 100 \quad (2)$$

where, X_c is the percent crystallinity, ΔH_m is the melting enthalpy of the polymer, ΔH_m^0 is the melting enthalpy of pure crystalline polymer ($\Delta H_m^0 = 146 \text{ Jg}^{-1}$), f_p is the weight fraction of the PHBV in the sample.

3.4. Thermo-Gravimetric Analysis (TGA)

TGA was carried out using a TA instrument Q500. The samples were heated up to 600°C from 30°C at a heating rate of 10°C/min. An inert atmosphere was

created using nitrogen gas at a rate of 40ml/min. The temperature at the onset of degradation; maximum degradation temperature (from the peak of the DTG curve) and the inorganic content (residue left at 600°C) were calculated.

3.5. Activation Energy Determination

The activation energy of decomposition was measured using Coats and Redfern model. According to this model, a graph of $\log [-\log (1-\alpha)/T^2]$ against $1000/T$ was plotted, where T is the temperature and α is the degree of conversion which can be found by following equation:

$$\alpha = \frac{(w_i - w_t)}{(w_i - w_f)} \quad (3)$$

where, w_i and w_f is the initial and final weight of samples and w_t is the weight at temperature T. A straight line from the graph is obtained and the activation energy (KJ) was calculated using equation 4.

$$E_a = \text{Slope} \times 2.303 R \quad (4)$$

where, R is the universal gas constant.

3.6. Tensile Properties

Tensile test was conducted according to ASTM D882-02 standard on a universal tensile testing machine MTS 793 at room temperature $25 \pm 2^\circ\text{C}$ using a crosshead speed of 12.5mm/min. A minimum of eight samples was tested. Tensile strength, modulus and strain at break of PHBV/HNTs samples were determined and compared with neat PHBV counterpart.

3.7. Microscopic Analysis

The surfaces of neat and PHBV/HNTs fractured samples were analyzed using a JEOL JSM-6400 scanning electron microscope (SEM) at an acceleration voltage of 15kV. A thin layer of gold was sputtered on the fractured surface of samples prior to SEM observation in order to increase the conductivity of the specimen.

4. RESULTS AND DISCUSSION

4.1. X-Ray Diffraction (XRD) Analysis

XRD patterns of pure HNT, pure PHBV and PHBV/HNT samples with various HNT concentrations are shown in Figure 2. The XRD patterns of HNT showed the basal peak at $2\theta = 12.1^\circ$ corresponding to a

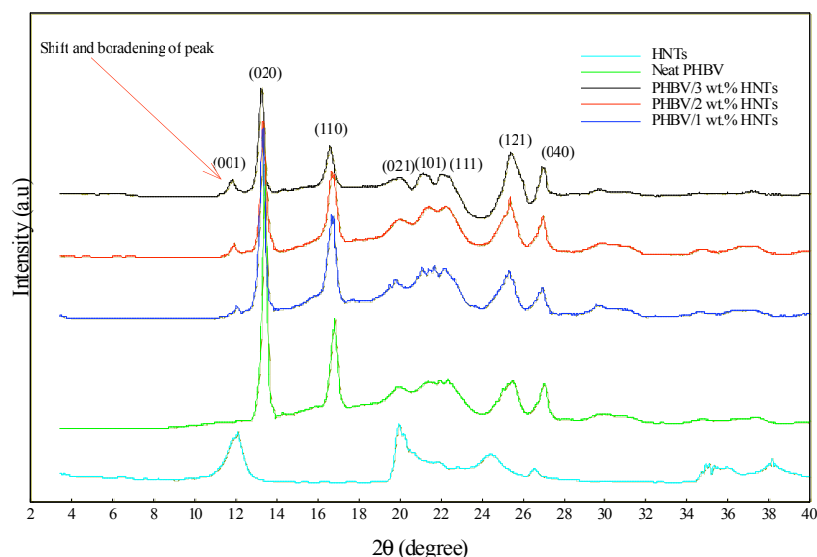


Figure 2: XRD plot of HNTs, Neat PHBV and PHBV/1-3 wt. % HNTs samples.

(001) basal spacing of 0.73nm this confirms the nanoscale size of the halloysites as well as the tubular structure of them [1, 14]. With the dispersion by extrusion method, it was seen that after the addition of HNTs in PHBV, the HNT internal channel diffraction peak at (001 plane) shifted to lower angle indicating a layer expansion of HNT tubes. From the results, it was found that the interlayer distance of the basal plane increased from 0.73nm in neat samples to 0.743nm, 0.747nm and 0.752nm in HNT-PHBV nanocomposites at 1, 2 and 3 wt.% loading. This increase in the interlayer spacing indicated that the PHBV was successfully intercalated inside the HNT layer. Also, it was observed from the XRD graph, that the intensity of the diffraction peak decreased and broaden in the nanocomposites compared to original halloysite clay indicating exfoliation of the HNTs in PHBV matrix. These results suggest that HNTs were homogeneously dispersed due to the strong interaction between the PHBV and HNT, which may have originated from hydrogen bonding between the carboxyl group of PHBV and hydroxyl group present in the inner side or at the edge of the HNTs [1, 16].

4.2. Crystallinity and Crystallite Dimension

XRD diffraction intensity of PHBV film at $2\theta=12.1^\circ$ shown in Figure 2 showed an increasing trend from neat PHBV to PHBV/HNTs with a maximum at 3 wt. % HNTs concentration. Also, the broadening of peak was found with increasing HNTs concentration. Also, with the addition of HNTs, diffractogram presented a better resolution for peaks at (021), (101), (111), (121) and (040) for PHBV/HNTs samples than neat PHBV. This increase in trend can be attributed to the fact that crystallization of PHBV was promoted by the addition of HNTs, which is also found in good agreement with the DSC data. It could also be said that crystalline growth of PHBV varied in different directions [23]. The increase in crystallinity can be attributed to the nucleation effect of HNTs [23].

Crystallochemical parameters derived from (020) and (110) reflection are reported in Table 1, showing full width half maximum ($\Delta^2\theta$) value (FWHM) and calculated the crystallite size of the sample. The crystallite size of the PHBV samples decreased with the addition of HNTs, which is due to the above

Table 1: Crystallite Size and Crystallite Dimension of Neat and PHBV/1-3 wt. % HNTs Samples

Sample	FWHM (°)	Crystallite Size (nm)	FWHM (°)	Crystallite Size (nm)
	(020)	(020)	(110)	(110)
Neat PHBV	0.3	1.98	0.34	1.40
PHBV/1 wt.% HNTs	0.32	1.87	0.35	1.37
PHBV/2 wt.% HNTs	0.38	1.58	0.38	1.27
PHBV/3 wt.% HNTs	0.39	1.55	0.4	1.22

mentioned nucleation effect. There are two predetermined factors that affect the size of the crystallites. The thermodynamics condition such as crystallization temperature and crystallization time, as well as the number of heterogeneous nucleation points. In this study, HNTs were considered as the heterogeneous nucleation points for PHBV chains. Due to small diameters of HNTs, the tubes can be considered as rigid macromolecules, thus PHBV polymer chains prefer to absorb and align on HNTs surface. Due to the nucleation effect of the HNTs, polymer started to crystallize on the surface of the HNTs. But then, geometric confinement became the major factor and thus affected the size of the crystallites. Therefore, HNTs can prevent the PHBV from growing into large size crystallites due to significantly increased number of nucleation points. As a result, decreased size of crystallites with higher crystallite density was obtained [24].

4.3. Differential Scanning Calorimetry (DSC) Analysis

DSC analysis was performed to study the effect of HNTs on the non-isothermal crystallization behavior of PHBV nanocomposites. The incorporation of HNTs influenced the crystallization, melting and recrystallization process as shown in Table 2. It is well known that the nanoparticles acts as heterogeneous nuclei and influences the crystallization process of polymers. As a result, the crystallization temperature was found higher in PHBV/HNTs samples in comparison to neat samples. Figure 3 illustrates the crystallization curve of PHBV/HNTs with different HNTs concentration. It is

Table 2: DSC Data of Neat and PHBV/1-3 wt. % HNTs Samples

Samples	$T_c(^{\circ}\text{C})$	$T_m(^{\circ}\text{C})$	$\Delta H(\text{J/g})$	Crystallinity(%)
Neat PHBV	102.75	150	53.30	36.51
PHBV / 1 wt.% HNTs	104.35	152	56.65	38.80
PHBV / 2wt.% HNTs	105.77	153	60.15	41.20
PHBV / 3 wt.% HNTs	106.21	154	66.66	45.66

clear from the results shown in Figure 3, that the crystallization onset and peak temperature increased consistently with increasing HNTs content. Also, from DSC data, it can be seen that the PHBV/HNTs composites are more crystalline than neat PHBV, which may be due to the lower nucleation density of nanocomposites. These results confirmed the results obtained from XRD data described in section 4.1. Better distribution of HNTs in the polymer matrix and strong interaction between them may have increased the crystallinity in PHBV/HNTs samples evident from the higher values of percent crystallinity (X_c).

Also, DSC results showed a complex behavior in all the samples during melting as shown in Figure 3. The melting process showed two different components during the endothermic heat reaction for both neat and PHBV/HNTs samples. It was found that the melting peak appeared at lower temperature followed by a presence of a shoulder of peak at higher temperatures. This shoulder became more visible and prominent with the addition of HNTs shown in Figure 3. Moreover, it

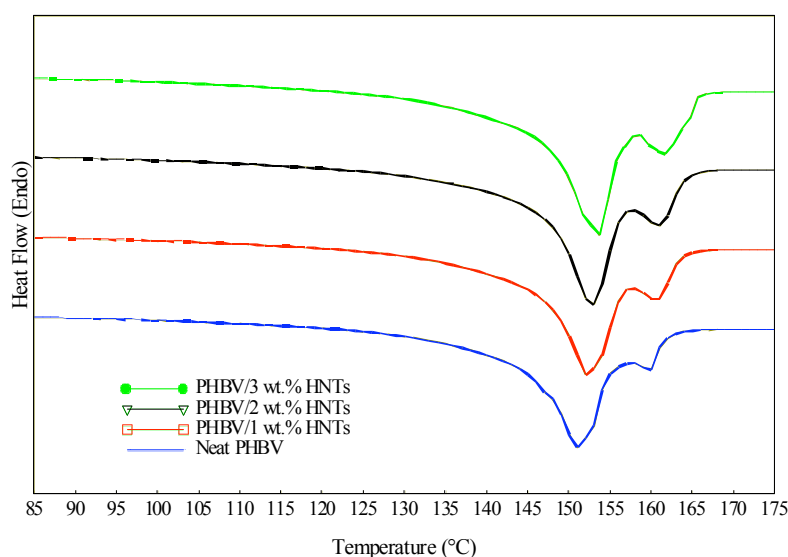


Figure 3: DSC curve of neat PHBV and PHBV/1-3 wt. % HNTs samples.

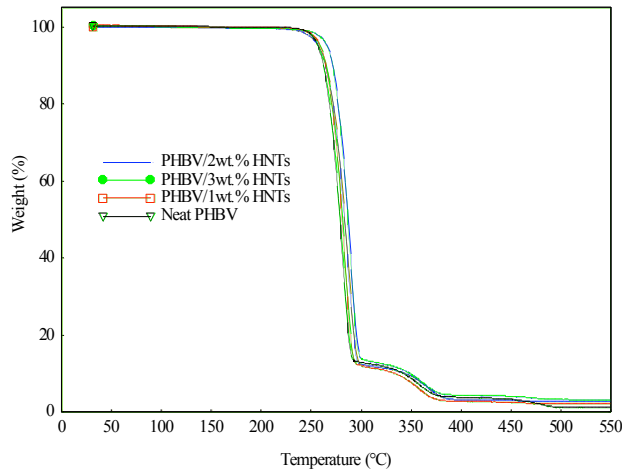


Figure 4: TGA curve of neat PHBV and PHBV/1-3 wt. % HNTs samples.

was also noticed that the temperature of the melting peak shifted slightly to higher temperature due to the addition of HNTs. The formation of a double melting peak in PHBV and PHBV/HNTs is due to the evaluation

of two crystalline phases of different order, size and thickness [1, 25]. Also, the increase in the melting temperature can be attributed to uniform dispersion of HNTs in the polymer. The bonding between HNTs and polymer tends to absorb more heat to melt, resulting in higher melting temperature. Moreover, the formation of a more arranged structure (crystalline) may have also affected the melting behavior.

4.4. Thermo-Gravimetric Analysis (TGA)

Thermogravimetric (TG) and the derivative thermogravimetric (DTG) curves of PHBV and PHBV/HNTs samples under nitrogen environment at a heating rate of 10°C/min are shown in Figures 4-5. It was found that the degradation of PHBV happened in two steps. The main degradation occurred at the temperature of 271°C, whereas, the second step degradation started around 360°C. This can be probably due to the fact that the monomers present in the samples may have evaporated at two different temperatures.

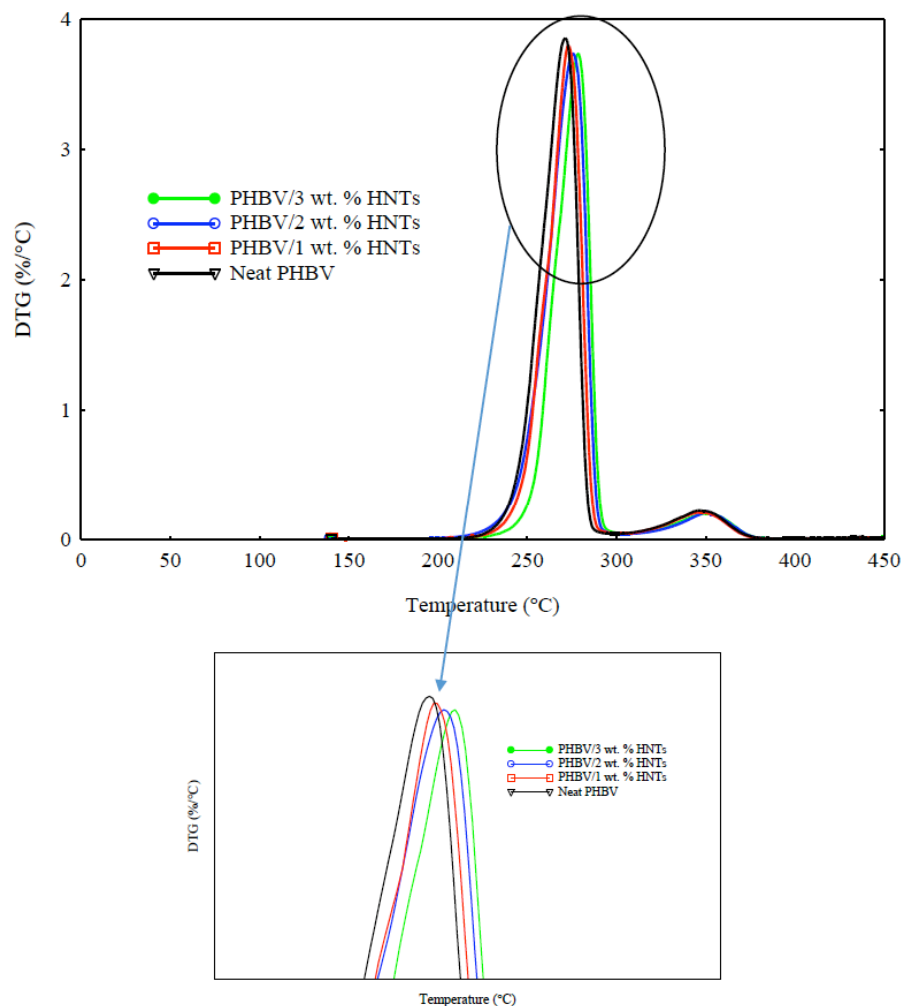


Figure 5: DTG curve of neat PHBV and PHBV/1-3 wt. % HNTs samples.

The characteristics of the TG and DTG curves where the onset temperature, T^0 (start of degradation), the temperature at which maximum rate of degradation occurs in first degradation step, T^m and the char content or residue left. The dependencies of the onset temperature, maximum degradation temperature and char content for neat and nanocomposites are shown in Table 3. From these results, the effect of HNTs on the PHBV properties can be clearly seen in comparison to neat samples. Data from the TGA curve revealed that the loading of HNTs played a major role in the thermal stability of nanocomposites. As shown in Table 3, the onset of degradation in neat PHBV samples occurred at a temperature of 271°C. However, this temperature for the 1-3 wt. % PHBV/HNTs samples increased to 273.53, 275.42 and 278.89°C respectively, which is 2.5, 4 and 7.8°C higher than neat PHBV samples. Temperature (T_m) where the maximum degradation occurs also showed a similar trend.

Table 3: TGA Data of Neat and PHBV/1-3 wt. % HNTs Samples

Sample	T(°C)	Maximum Decomposition Temp. (°C)	Char Content Left (%)
Neat PHBV	262.74	271.03	1.21
PHBV+1 wt% HNTs	265.47	273.53	2.03
PHBV+2 wt% HNTs	266.79	275.42	2.72
PHBV+3 wt% HNTs	268.65	278.89	3.11

The reason for this enhancement can be attributed to good dispersion of the HNTs in the PHBV polymer which may have favored: (i) formation of a tortuous diffusion path for the released degradation products, and (ii) the entrapment of volatile products at the surface and inside the hollow tubular structure of HNTs. Both of these effects hindered the out-diffusion of volatile decomposition products which resulted in an effective delay of the mass transfer and an increased thermal stability of PHBV matrix [26].

4.5. Activation Energy

The activation energy is related with thermal stability. The higher activation energy indicates higher thermal stability. The activation energy for the thermal

degradation of neat PHBV and PHBV/HNTs samples were determined from the plot of $-\log[-\log(1-\alpha)/T^2]$ against $1000/T$. From Figure 6 and Table 4, it can be seen that the amount of activation energy needed for thermal degradation increased with increasing concentration of HNTs content. This increased in activation energy can also be attributed to the increase in thermal stability of PHBV/HNTs samples.

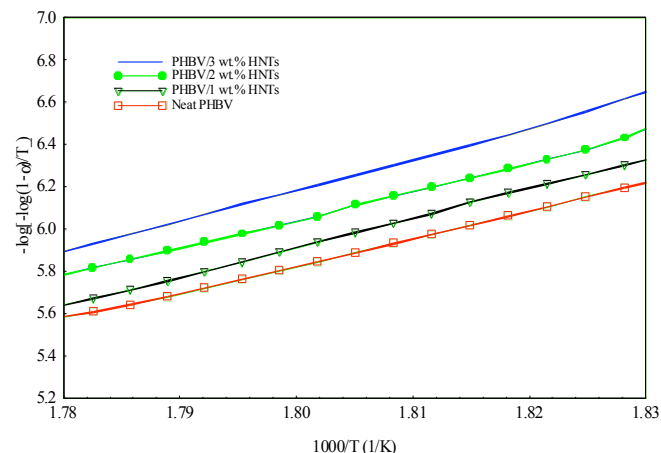


Figure 6: Activation energy of neat PHBV and PHBV/1-3 wt. % HNTs samples (Coats and Redfern model).

Table 4: Activation Energy of Neat and PHBV/1-3 wt. % HNTs Samples

Sample	Activation Energy, E (KJ/mole)
Neat PHBV	252.92
PHBV+1 wt.% HNTs	268.66
PHBV+2 wt.% HNTs	290.34
PHBV+3 wt.% HNTs	309.20

4.6. Tensile Properties

Figure 7 shows the effect of HNTs content on the tensile strength of neat PHBV and PHBV/HNTs samples. The addition of HNTs increased the tensile strength linearly with the increase in HNTs concentration. The PHBV samples at 3 wt. % HNTs loading exhibited 21% increase in tensile strength in comparison to neat samples. This increase in tensile strength could be due to various factors. Better dispersion of HNTs inside PHBV, inter tubular interaction between HNTs and the PHBV, the edge to edge and face to face interaction between HNTs which formed a zig-zig structures as well as three dimensional orientations of HNTs inside the

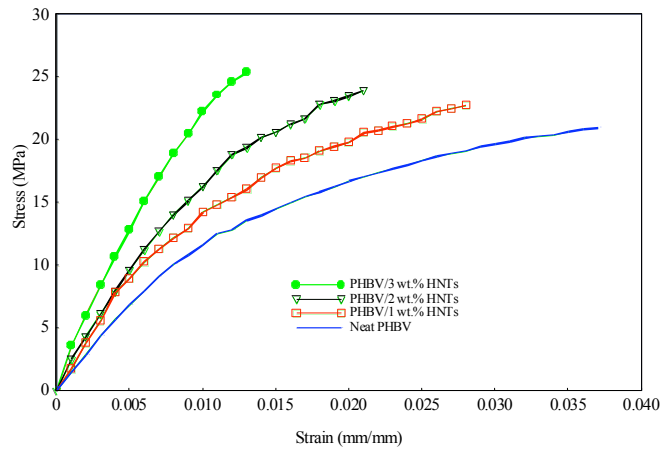


Figure 7: Tensile stress-strain curve of neat PHBV and PHBV/1-3 wt. % HNTs samples.

nanocomposites. Hedicke–Hochstotter *et al.* [26] found improvement in both strength and stiffness using

unmodified HNT and according to them, higher intrinsic stiffness of the nanotubes and interactions with polymer matrix were attributed to this improvement. As stated by Pavlidou and Papaspyrides [27], the improvement in mechanical properties of polymeric nanocomposites depends on the proper dispersion of nanoparticle in a polymer matrix and on the intercalation/exfoliation ratio.

The tensile modulus of PHBV samples increased significantly with HNT content shown in Table 5. The tensile modulus increased linearly by 54% for 3wt. % HNTs added PHBV samples when compared to neat PHBV counterpart. Better dispersion of HNTs and increased interfacial adhesion between the filler and polar PHBV polymer can be attributed to a significant increase in stiffness.

Table 5: Tensile Properties of Neat and PHBV/1-3 wt. % HNTs Samples

Sample	Tensile Strength, (MPa)	% Increase	Young's Modulus (MPa)	% Increase	Elongation at Break
Neat PHBV	20.95± 0.07	-	1665± 47	-	0.037
PHBV/1 wt.% HNTs	22.74± 0.07	+8.5	1890± 155	+13.4	0.028
PHBV/2 wt.% HNTs	23.92± 0.9	+14	2120± 113	+27.4	0.021
PHBV/3 wt.% HNTs	25.37± 0.46	+21	2573± 61	+54	0.013

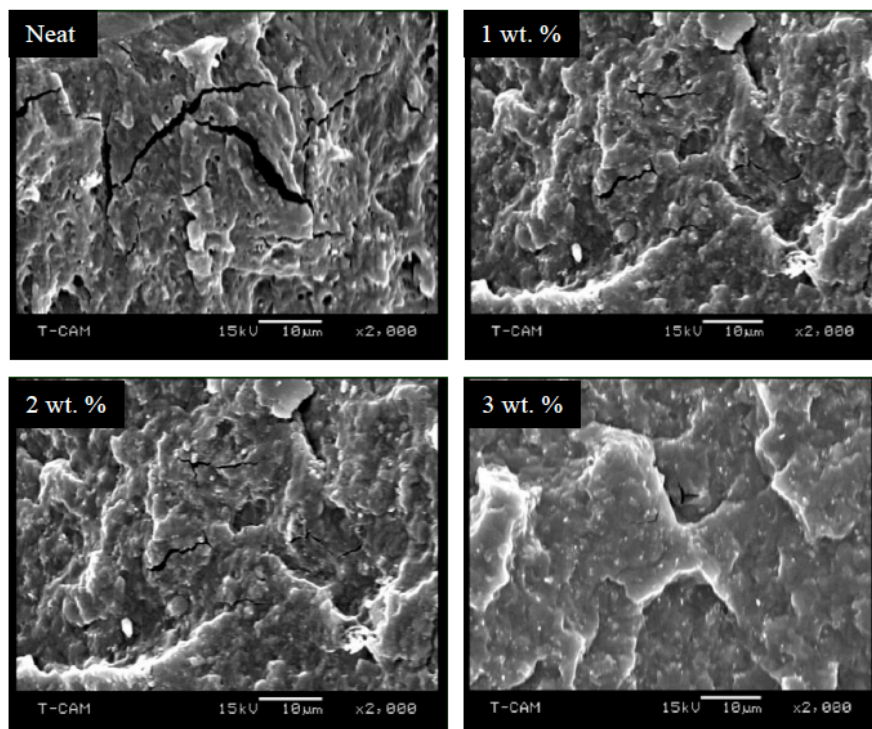


Figure 8: SEM micrographs of tensile fractured specimens, (a) neat, (b) 1 wt. %, (c) 2 wt. % and, (d) 3 wt. % PHBV/HNTs.

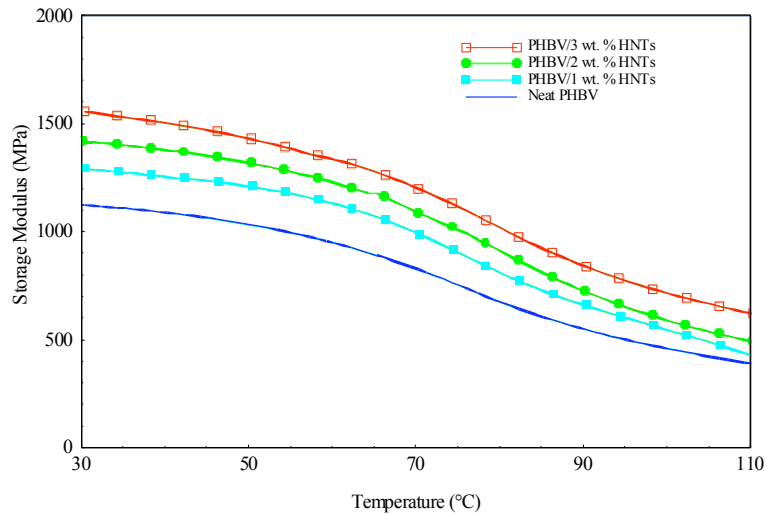


Figure 9: Storage modulus vs. temperature response of neat PHBV and PHBV/1-3 wt. % HNTs samples.

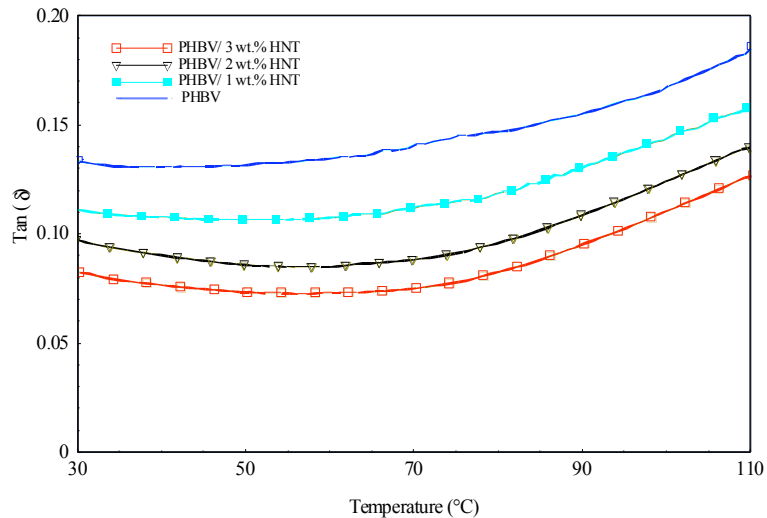


Figure 10: Tan δ vs. temperature response of Neat PHBV and PHBV/1-3 wt. % HNTs samples.

4.7. Microscopic Analysis

Figure 8 shows a scanning electron micrographs (SEM) of tensile tested samples. The micrographs revealed presence of cracks and microvoids in the neat PHBV samples. On the other hand, it was seen that the PHBV samples with increasing HNT content showed the presence of less cracks shown in Figure 8. Also, the length of the cracks was reduced considerably in the nanocomposites compared to neat PHBV. The strong reinforcing effect may have prevented the formation of micro voids and crack growths. The strong interaction between HNTs and PHBV polymer may have contributed to the reinforcing effect by preventing debonding of the particles. Also, it was seen from micrographs, that the PHBV/HNTs samples showed surface with the brittle nature compared to the neat

one. This result matched well with the tensile results. The infusion of HNTs increased the rigidity of the matrix and increased the brittleness of PHBV composites, which resulted in a decrease in strain to failure in PHBV/HNTs samples in comparison to neat one.

4.8. Dynamic Mechanical Analysis (DMA)

The viscoelastic properties of PHBV and PHBV-HNT nanocomposites were studied using DMA analysis. The storage modulus, loss modulus and tan delta with respect to temperature is shown in Figures 9-10 and Table 6. The storage modulus denotes the elastic nature of a polymeric composite and the loss modulus indicates the plastic nature or energy dissipated during heating of a polymeric nanocomposite. The higher the storage modulus, the better the stiffness of a nanocomposite and better the

Table 6: DMA of Neat and PHBV/1-3 wt. % HNTs Samples

Sample	PHBV	PHBV+1 wt. % HNTs	% Change	PHBV+2 wt. % HNTs	% Change	PHBV+3 wt. % HNTs	% Change
Storage modulus. at 30°C (MPa)	1135±12	1280±27	+13	1417±22	+25	1557±16	+37
Tan δ	0.135	0.110	-	0.0972	-	0.0823	-
Loss Modulus (MPa)	153.23±07	142.10	-7	137.50±12	-10	128.12±15	-16

response with respect to temperature. The storage modulus increased linearly with the optimal increase of 37% in PHBV/3 wt. % sample in comparison to neat samples shown in Table 6. Better dispersion of HNTs into the polymer matrix may have restricted the polymer chain mobility, and thus improved the stiffness of the polymer. However, the loss factor, $\tan \delta$, was found to decrease with the addition of HNTs with the lowest in 3 wt. % HNTs loading samples in comparison to neat PHBV samples as shown in Table 6. The $\tan \delta$ provides the account of energy dissipated as heat during the dynamic testing [28]. Higher $\tan \delta$ value in neat PHBV samples can be attributed to more energy dissipation in the samples. In contrast, the decrease in loss factor in PHBV/HNTs samples can be attributed to a higher degree of crystallinity. Crystalline structures reduce the loss modulus giving rise to the storage modulus. Loss modulus is related to the molecular chain mobility of the polymer. The lower loss modulus in PHBV/HNTs samples in comparison to neat PHBV samples evident from Table 6 can be attributed to the nanotubes and improved interfacial bonding between the HNTs and PHBV which may have imposed restriction on the expansion of the molecular chain in the amorphous region.

CONCLUSION

The objective of this study was to see the change in mechanical and thermal properties of a biodegradable polymer PHBV with the reinforcement of HNTs. It was found that the PHBV polymer was well exfoliated and intercalated inside HNT tubes confirming good dispersion of HNTs. DSC analysis indicated that incorporation of HNTs positively affected the crystallization kinetics and increased the crystallinity of PHBV/HNTs samples due to the nucleation effect of HNTs. Also, it increased the melting temperature of the PHBV/HNTs samples, indicating improved thermal stability of nanobiocomposites. Moreover, the incorporation of small amounts of HNTs showed

improvement in tensile strength and stiffness with a compromise in strain to failure. It is concluded that the HNTs can be effectively used as a reinforcing nanoparticle for improving the mechanical and thermal properties of biodegradable PHBV nanobiocomposites.

ACKNOWLEDGEMENT

The authors acknowledge the financial support of NSF-CREST Grant No. HRD 1137681, NSF Grant No. HRD-1409918, NSF-EPSCoR Grant No. EPS-1158862 and NSF-REU Grant No. DMR-1358998 for this research work.

REFERENCES

- [1] Carli LN, Crespo JS and Mauler RS. Composites : Part A PHBV nanocomposites based on organomodified montmorillonite and halloysite : The effect of clay type on the morphology and thermal and mechanical properties. *Composites Part A* 2011; 42(11): 1601-1608. <http://dx.doi.org/10.1016/j.compositesa.2011.07.007>
- [2] Xie Y, Kohls D, Noda I, Schaefer DW, Akpalu YA. Poly (3-hydroxybutyrate- co -3-hydroxyhexanoate) nanocomposites with optimal mechanical properties. *Polymer*. 2009; 50(19): 4656-4670. <http://dx.doi.org/10.1016/j.polymer.2009.07.023>
- [3] Singh S, Mohanty AK, Sugie T, Takai Y. Renewable resource based biocomposites from natural fiber and polyhydroxybutyrate-co-valerate (PHBV) bioplastic. 2008; 39: 875-886. <http://dx.doi.org/10.1016/j.compositesa.2008.01.004>
- [4] Javadi A, Srithep Y, Clemons CC, Turng L-S, Gong S. Processing of poly(hydroxybutyrate-co-hydroxyvalerate)-based bionanocomposite foams using supercritical fluids. *Journal of Materials Research*. 2012; 27(11): 1506-1517. <http://dx.doi.org/10.1557/jmr.2012.74>
- [5] Chen GX, Hao GJ, Guo TY, Song MD, Zhang BH. Crystallization Kinetics of Poly(3-Hydroxybutyrate-co-3-Hydroxyvalerate)/Clay Nanocomposites. *J Appl Polym Sci*. 2004; 93: 655-661. <http://dx.doi.org/10.1002/app.20512>
- [6] Zainuddin S, Hosur M V., Zhou Y, Narteh AT, Kumar A, Jeelani S. Experimental and numerical investigations on flexural and thermal properties of nanoclay-epoxy nanocomposites. *Materials Science and Engineering A*. 2010; 527(29-30): 7920-7926. <http://dx.doi.org/10.1016/j.msea.2010.08.078>
- [7] Rahman MM, Hosur M, Zainuddin S, Jajam KC, Tippur H V., Jeelani S. Mechanical characterization of epoxy composites modified with reactive polyol diluent and randomly-oriented

- amino-functionalized MWCNTs. *Polymer Testing*. 2012; 31(8): 1083-1093. doi:10.1016/j.polymeresting.2012.08.010. <http://dx.doi.org/10.1016/j.polymeresting.2012.08.010>
- [8] Zainuddin S, Fahim a., Arifin T, et al. Optimization of mechanical and thermo-mechanical properties of epoxy and E-glass/epoxy composites using NH₂-MWCNTs, acetone solvent and combined dispersion methods. *Composite Structures*. 2014; 110(1): 39-50. <http://dx.doi.org/10.1016/j.compstruct.2013.11.010>
- [9] Zainuddin S, Hosur M V., Zhou Y, Kumar A, Jeelani S. Durability studies of montmorillonite clay filled epoxy composites under different environmental conditions. *Materials Science and Engineering A*. 2009; 507(1-2): 117-123. <http://dx.doi.org/10.1016/j.msea.2008.11.058>
- [10] Rahman MM, Zainuddin S, Hosur M V., et al. Improvements in mechanical and thermo-mechanical properties of e-glass/epoxy composites using amino functionalized MWCNTs. *Composite Structures*. 2012; 94(8): 2397-2406. <http://dx.doi.org/10.1016/j.compstruct.2012.03.014>
- [11] Hosur M, Barua R, Zainuddin S, Kumar A, Trovillion J, Jeelani S. Effect of processing techniques on the performance of Epoxy/MWCNT nanocomposites. *Journal of Applied Polymer Science*. 2013; 127(6): 4211-4224. <http://dx.doi.org/10.1002/app.37990>
- [12] Rahman MM, Zainuddin S, Hosur M V., et al. Effect of NH₂-MWCNTs on crosslink density of epoxy matrix and ILSS properties of e-glass/epoxy composites. *Composite Structures* 2013; 95: 213-221. <http://dx.doi.org/10.1016/j.compstruct.2012.07.019>
- [13] Kamble R, Ghag M, Gaikawad S nad Panda BK. *Journal of Advanced Scientific Research Halloysite Nanotubes and Applications: A Review*. *J Adv Scient Res Journal of Advanced Scientific Research* 2012; 3(32): 25-29. Available at: <http://www.sciensage.info/jasr>.
- [14] Yuan P, Southon PD, Liu Z, et al. Functionalization of halloysite clay nanotubes by grafting with aminopropyltriethoxysilane. *Journal of Physical Chemistry C*. 2008. <http://dx.doi.org/10.1021/jp805657i>
- [15] Ismail H, Shaari SM. Curing characteristics, tensile properties and morphology of palm ash/halloysite nanotubes/ethylene-propylene-diene monomer (EPDM) hybrid composites. *Polymer Testing*. 2010. <http://dx.doi.org/10.1016/j.polymeresting.2010.04.005>
- [16] Du M, Guo B, Lei Y, Liu M, Jia D. Carboxylated butadiene-styrene rubber/halloysite nanotube nanocomposites: Interfacial interaction and performance. *Polymer*. 2008. <http://dx.doi.org/10.1016/j.polymer.2008.08.042>
- [17] Soheilmooghaddam M, Wahit MU, Mahmoudian S, Hanid NA. Regenerated cellulose/halloysite nanotube nanocomposite films prepared with an ionic liquid. *Materials Chemistry and Physics*. 2013. <http://dx.doi.org/10.1016/j.matchemphys.2013.06.029>
- [18] Prashantha K, Lacrampe MF, Krawczak P. Processing and characterization of halloysite nanotubes filled polypropylene nanocomposites based on a masterbatch route: Effect of halloysites treatment on structural and mechanical properties. *Express Polymer Letters*. 2011. <http://dx.doi.org/10.3144/expresspolymlett.2011.30>
- [19] Zhao M, Liu P. Halloysite nanotubes/polystyrene (HNTs/PS) nanocomposites via in-situ bulk polymerization. *Journal of Thermal Analysis and Calorimetry* 2008; 94: 103-107. <http://dx.doi.org/10.1007/s10973-007-8677-4>
- [20] Marney DCO, Russell LJ, Wu DY, et al. The suitability of halloysite nanotubes as a fire retardant for nylon 6. *Polymer Degradation and Stability*. 2008; 93(10): 1971-1978. <http://dx.doi.org/10.1016/j.polymdegradstab.2008.06.018>
- [21] Sanchez-Garcia MD, Lagaron JM, Hoa S V. Effect of addition of carbon nanofibers and carbon nanotubes on properties of thermoplastic biopolymers. *Composites Science and Technology*. 2010; 70(7): 1095-1105. <http://dx.doi.org/10.1016/j.compscitech.2010.02.015>
- [22] Ten E, Turtle J, Bahr D, Jiang L, Wolcott M. Thermal and mechanical properties of poly(3-hydroxybutyrate-co-3-hydroxyvalerate)/cellulose nanowhiskers composites. *Polymer*. 2010; 51(12): 2652-2660. <http://dx.doi.org/10.1016/j.polymer.2010.04.007>
- [23] Lai M, Li J, Yang J, Liu J, Tong X, Cheng H. The morphology and thermal properties of multi-walled carbon nanotube and poly(hydroxybutyrate-co-hydroxyvalerate) composite. *Polymer International*. 2004; 53(10): 1479-1484. <http://dx.doi.org/10.1002/pi.1566>
- [24] Yu HY, Qin ZY, Zhou Z. Cellulose nanocrystals as green fillers to improve crystallization and hydrophilic property of poly(3-hydroxybutyrate-co-3-hydroxyvalerate). *Progress in Natural Science: Materials International*. 2011; 21(6): 478-484. [http://dx.doi.org/10.1016/S1002-0071\(12\)60086-0](http://dx.doi.org/10.1016/S1002-0071(12)60086-0)
- [25] Chen H, Zheng M, Sun H, Jia Q. Characterization and properties of sepiolite/polyurethane nanocomposites. *Materials Science and Engineering A*. 2007; 445-446: 725-730. <http://dx.doi.org/10.1016/j.msea.2006.10.008>
- [26] Hedicke-Höchstötter K, Lim GT and Altstädt V. Novel polyamide nanocomposites based on silicate nanotubes of the mineral halloysite. *Composites Science and Technology* 2009; 69(3-4): 330-334. <http://dx.doi.org/10.1016/j.compscitech.2008.10.011>
- [27] Pavlidou S, Papispyrides CD. A review on polymer-layered silicate nanocomposites. *Progress in Polymer Science (Oxford)* 2008; 33(12): 1119-1198. <http://dx.doi.org/10.1016/j.progpolymsci.2008.07.008>
- [28] Group F, Avenue M, Square P, Park M and Ox O. Library of Congress Cataloging-in-Publication Data Visit the Taylor and Francis Web site at; 2005.

Received on 04-04-2016

Accepted on 27-06-2016

Published on 14-10-2016

DOI: <http://dx.doi.org/10.15377/2410-4701.2016.03.01.2>© 2016 Fahim *et al.*; Avanti Publishers.

This is an open access article licensed under the terms of the Creative Commons Attribution Non-Commercial License (<http://creativecommons.org/licenses/by-nc/3.0/>) which permits unrestricted, non-commercial use, distribution and reproduction in any medium, provided the work is properly cited.